2D DIFFUSE OPTICAL IMAGING USING CLUSTERED SPARSITY

Chen Chen[1]*, Fenghua Tian*[2]*, Jixing Yao*[3]*, Hanli Liu*[2] *and Junzhou Huang*[1]

[1]Department of Computer Science and Engineering, University of Texas at Arlington
[2]Department of Bioengineering, University of Texas at Arlington
[3]Department of Electrical Engineering, University of Texas at Arlington

ABSTRACT

Diffuse optical imaging (DOI) is a non-invasive technique which measures hemodynamic changes in the tissue with near infrared light, and has been increasingly used to study brain functions. Due to the nature of light propagation in the tissue, the reconstruction problem is severely ill-posed. Sparsity-regularization has achieved promising results in recent works for linearized DOI problem. In this paper, we exploit more prior information to improve DOI besides sparsity. Based on the functional specialization of the brain, the in vivo absorption changes caused by specific brain function can be clustered in certain region(s) and not randomly distributed. Thus, a new algorithm is proposed to utilize this prior in reconstruction. Results of numerical simulations and phantom experiments have demonstrated the superiority of the proposed method over the state-of-the-art.

Index Terms— diffuse optical tomography, sparsity regularization, overlapping group sparsity, clustered sparsity

1. INTRODUCTION

Diffuse optical imaging (DOI) is an emerging technique to study brain functions due to its non-invasive manner and relatively low cost. This technique uses near infrared light in a range of 650 to 900 nm, which is sensitive to the absorptions of oxygenated hemoglobin (HbO2) and deoxygenated hemoglobin (Hb). The light sources and detectors are arranged on the scalp. The diffused light from the cortical layer of the brain is acquired to form an image of activation.

One of the main challenges in DOI is the image reconstruction (or inverse problem). Due to the diffusive nature of light and limited numbers of sources and detectors, the inverse problem is severely ill-posed. After necessary linearization approximation, regularization is often applied to the inverse problem to obtain unique solution. Conventionally, the ℓ_2-norm regularization (also known as Tikhonov regularization) is the mostly used method because it can be easily implemented. The drawback is its tendency to over-smooth the image by penalizing large values.

As the perturbation from a homogeneous background or reference medium is relatively small in volume and contrast, sparsity of the reconstructed image is generally assumed in recent methods [1][2][3][4]. Guided by compressive sensing theory [5], if this prior information is utilized, signal or image can be recovered from far fewer measurements than that dictated by Shannon-Nyquist theorem under mild conditions. In these works, regularization with sparsity inducing norm, such as ℓ_1, ℓ_p $(0 < p < 1)$ and smooth-ℓ_0, has shown promising results over the conventional ℓ_2 norm.

It is widely known that human actions correspond to certain regions of brain activation. For example, brain state changes specifically in the dorsal medial prefrontal area during Vipassana meditation [6]. These changes of brain state only take place in a region or regions but not randomly distributed over the whole brain, which will make the change of absorption have a clustered appearance. In contrast to previous works, we propose a new method to improve the reconstruction by exploiting this prior information. According to structured sparsity theories [7][8], fewer measurements are required for signals with clustered sparsity than those with standard sparsity, or recovery accuracy can be improved with the same number of measurements. A novel algorithm is proposed to solve this problem based on the Fast Iterative Shrinkage-Thresholding Algorithm (FISTA) framework [9]. Experimental results has demonstrated the significant improvements achieved by our method when compared with previous works.

2. RELATED WORK

The relative change in optical density is measured by each source-detector (S-D) pair. By Rytov approximation, the reconstruction problem in DOI can be formulated as [3]:

$$Ax = b \tag{1}$$

where $b \in \mathbb{R}^{m\times 1}$ is the vector of measured relative light density changes; $x \in \mathbb{R}^{n\times 1}$ represents an image (after vectorizing) of $\triangle\mu_a$ (i.e. the change of absorption); $A \in \mathbb{R}^{m\times n}$ is the forward sensing matrix referring to the sensitivity of pixels with different S-D pairs. Due to the limitation on number of S-D pairs and diffusive nature of light, this problem is severely ill-posed, i.e. $m << n$. To obtain unique solution, ℓ_2-norm regularization is widely used and the objective

978-1-4673-1961-4/14/$31.00

function becomes [10]:

$$\hat{x} = \arg\min_x \{\frac{1}{2}||Ax - b||_2^2 + \lambda||x||_2^2\} \quad (2)$$

where λ is a positive parameter and selected by an L-curve algorithm [11]. To overcome the over-smoothing by ℓ_2-norm regularization, many recent methods have been proposed to exploit the sparsity of the reconstructed image [1][3][4]. Sparsity-inducing norms, e.g. ℓ_1, ℓ_p $(0 < p < 1)$ and smooth-ℓ_0 norms, are used for regularization instead of ℓ_2 norm:

$$\hat{x} = \arg\min_x \{\frac{1}{2}||Ax - b||_2^2 + \lambda||x||_p^p\} \quad (3)$$

and

$$\hat{x} = \arg\min_x \{\frac{1}{2}||Ax - b||_2^2 + \lambda||x||_0\} \quad (4)$$

where the ℓ_0 norm is approximated with Gaussian function. Promising results have been obtained using these methods. However, these standard sparsity based methods only exploit the sparseness of the reconstructed image, while the correlations of the non-zero values have not been utilized.

3. ALGORITHM

As mentioned above, the in vivo absorption change caused by functional brain activation will be clustered in certain regions of the brain but not randomly distributed, which will result in a clustered appearance on the reconstructed image. Motivated by this prior information, we model the reconstruction problem as overlapping group sparsity (OGS) regularization [12]:

$$\hat{x} = \arg\min_x \{\frac{1}{2}||Ax - b||_2^2 + \lambda||x||_{2,1}\} \quad (5)$$

where the mixed $\ell_{2,1}$ norm is the summation of the group-wise ℓ_2 norms, i.e. $\ell_{2,1} = \sum_g ||x_g||_2$. g denotes one of the group and x_g denotes the entries in this group. We pre-define that each pixel and its surrounding pixels (e.g. 4, 8) are assigned into one group, which encourages sparsity and also encourages the non-zero pixels to cluster together in the reconstructed image [12]. By structured sparsity theories [7][8], it has been proved that only $\mathcal{O}(k + C\log(n/C))$ measurements are required to recovery clustered sparse signal instead of $\mathcal{O}(k + k\log(n/k))$ for standard sparse signal. Here k denotes the number of non-zeros entries of the signal and C denotes the number of clusters with $C << k$. With the same number of measurements, significant improvement can be gained by clustered sparsity. Note that this method can be combined with other regularization terms (if found in future) in the composite splitting algorithms framework [13].

To solve (5), we propose a new algorithm based on the FISTA [9] framework, which has been proved to reach optimal convergence rate for first order gradient methods. The whole algorithm is summarized in Algorithm 1. We call it as OGS reconstruction. For the first step, $f(x) = \frac{1}{2}||Ax - b||_2^2$ and $\nabla f(x) = A^T(Ax - b)$ denotes its gradient which has Lipschitz constant L. The smallest Lipschitz constant L can be selected based on the maximum eigenvalue of A^TA. A^T denotes the transpose of A. In the original FISTA algorithm for ℓ_1 norm regularization, the second step has closed form solution by soft-thresholding. However, due to the non-smoothness and non-separability of the overlapped $\ell_{2,1}$ norm, there is no closed form solution for the OGS thresholding/denosing problem in the second step. We apply a very fast algorithm [14] to solve it. Finally, each x^k is updated by the results in previous two iterations to accelerate the convergence.

Algorithm 1 OGS Reconstruction

Purpose: $\min_x\{\frac{1}{2}||Ax - b||_2^2 + \lambda||x||_{2,1}\}$
Input: $\rho = \frac{1}{L}$, λ, $t^1 = 1$, $y^0 = x^0$
for $k = 1$ **to** N **do**
1) $s = x^k - \rho\nabla f(x^k)$
2) $y^k = \arg\min_y\{\frac{1}{2\rho}\|y - s\|^2 + \lambda\|y\|_{2,1}\}$
3) $t^{k+1} = [1 + \sqrt{1 + 4(t^k)^2}]/2$
4) $x^{k+1} = y^k + \frac{t^k - 1}{t^{k+1}}(y^k - y^{k-1})$
end for

4. EXPERIMENT

4.1. Simulation

Simulations are conducted using PMI Toolbox [15]. The matrix A is generated by Rytov approximation [3]. The probe geometry is the same with that in previous work [16] and later phantom experiments. Given the ground truth image x^*, the measurement with $m = 188$ is generated by $b = Ax^* + e$, where e denotes the Gaussian noise with standard derivation σ. The field of view (FOV) is $6cm \times 6cm$ with resolution 61×61 pixels. Root-mean-square error (RMSE) and Contrast-to-Noise Ratio (CNR) [10] are used as metrics for evaluation. The reconstructed image with larger CNR means better performance. As suggested in [4], p is set as 0.5.

The RMSEs for different λ are presented at Figure 1 when $\sigma = 0.02\%$. Compared with previous methods, smaller errors are achieved by the proposed method with a proper λ, which coincides with the conclusion of structured sparsity theories. Both the ℓ_2 norm regularization [10] and the proposed method are less sensitive to the parameter setting.

Figure 2 presents the reconstruction results at the optimal parameters corresponding to Figure 1. All the reconstructed image are shown at the same scale. The absorbers reconstructed by ℓ_2 norm regularization [10] have low contrast to the background due to over-smoothing. Sparse results are achieved by smooth ℓ_0, $\ell_{0.5}$ [4] and ℓ_1 norm regularization [3], which have much higher contrast compared with the previous one. However, these norms only encourage sparsity

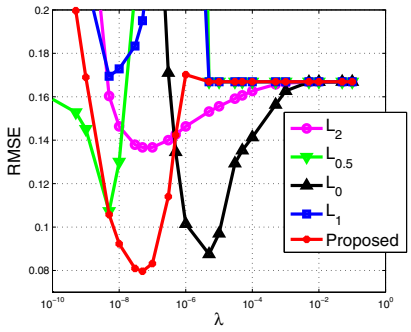

Fig. 1. Reconstruction performance of different algorithms when $\sigma = 0.02\%$. The minimum RMSEs for ℓ_2 [10], $\ell_{0.5}$ [4], smooth ℓ_0 [4], ℓ_1 [3] and the proposed are 0.136, 0.107, 0.087, 0.169 and 0.079 respectively.

and have no other constraints on the locations of the non-zero values. The absorbers on the images are slightly distorted and distributed. Our method not only induces sparsity, but also encourage the non-zero values to be clustered. The benefit of our penalty can be obviously found.

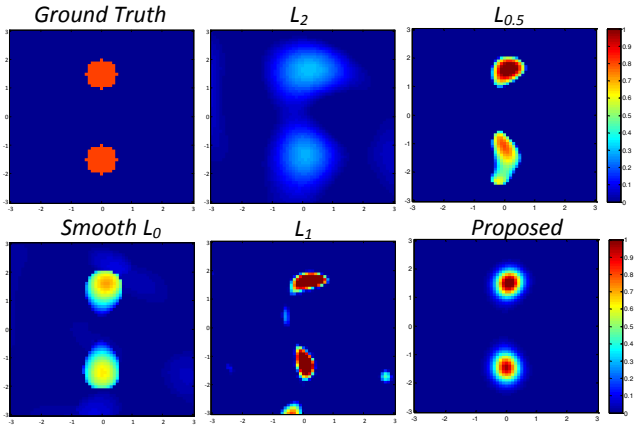

Fig. 2. The ground-truth image and the reconstructed images for the simulation. The CNRs of reconstructed images by ℓ_2 norm, $\ell_{0.5}$ norm, smooth ℓ_0 norm, ℓ_1 norm and the proposed are 3.16, 5.68, 8.03, 5.47 and **9.63** respectively.

We also validate these algorithms at noiseless case (i.e. $\sigma = 0$). All algorithms perform much better. From the visual results, the proposed method is still the closest to the ground-truth. When we increasing σ from 0 to 0.001, the reconstructed image of smooth ℓ_0 norm regularization tends to be similar as ℓ_2 norm regularization, with low contrast to the background. The results by $\ell_{0.5}$ and ℓ_1 are becoming severely distorted to lines. It is because standard sparsity based methods are sensitive to noise. However, the result by our method is only sightly distorted and the shapes of the absorbers can be clearly observed. Due to page length limitation, we do not display these results in details here.

4.2. Phantom

We further conduct experiments to validate our method using laboratory tissue phantoms. The experiment environment is the same as that in previous work [16]. A 1-cm-diameter spherical absorber with $\mu_a = 0.3$ cm^{-1} was placed around the x-axis and 3 cm below the surface of the phantom. The measured data with and without the absorber were respectively acquired by all of the 188 channels. Keeping the experimental setup, we then place a two spherical absorbers with 1 cm diameter around the y-axis with the same depth to conduct another experiment. Parameters for different algorithms are selected by the L-curve algorithm [10][3].

Figure 3 and 4 present the reconstruction results in these two phantom experiments. Similar tendency can be found as those in simulations. The images reconstructed by our method have the fewest artifacts, while some significant noise may be mistakenly recognized as true signal by standard sparsity methods. Reconstruction of the second data (Figure 4) is quite difficult as it is less sparse. The true absorbers are hard to be distinguished by $\ell_{0.5}$ and ℓ_1 norm methods. However, the proposed method still can recover the absorbers clearly, with much higher contrast than that by ℓ_2 or smooth ℓ_0 norm regularization. Quantitative comparisons of these experiments are listed in Table 1.

Table 1. CNR comparisons of the phantom experiments.

	ℓ_2	$\ell_{0.5}$	smooth ℓ_0	ℓ_1	Proposed
Figure 3	3.91	3.63	9.39	4.05	**12.71**
Figure 4	3.10	4.04	5.30	1.98	**6.73**

4.3. Discussion

The structured prior information has already been successfully used in computer vision and MRI [17][18][19][20]. Similarly, our method can improve the reconstruction as absorbers have clustered tendency. No additional information (e.g. shape, location of the absorbers) is required. It leads to several advantages: 1) improving the reconstruction accuracy with the same number of measurements; 2) maintaining stable recovery when the measurements are not sufficient for standard sparsity (e.g. by ℓ_1 norm); 3) enhancing the robustness to noise and preventing artifacts in the background.

5. CONCLUSION

By observing the clustered prior information in brain activation, we have proposed a new method to reconstruct diffuse optical image, whose performance is guaranteed by structured sparsity theories. Numerical simulation and phantom experiments have validated its effectiveness when compared with conventional and recent algorithms. Clinic applications can benefit from our method with few or no revision on the hardware. Future work will focus on non-convex $\ell_{2,p}$ norm regularization with $0 < p < 1$ to further improve reconstruction.

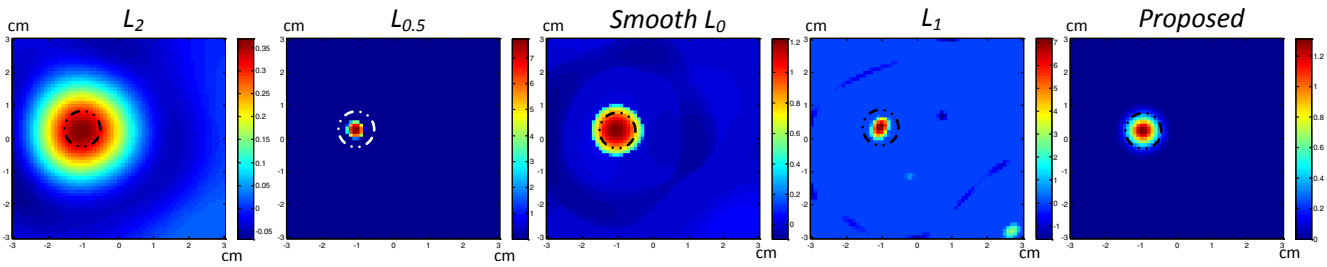

Fig. 3. Reconstructed images of a single absorber. Dashed circle indicates the actual size of the object.

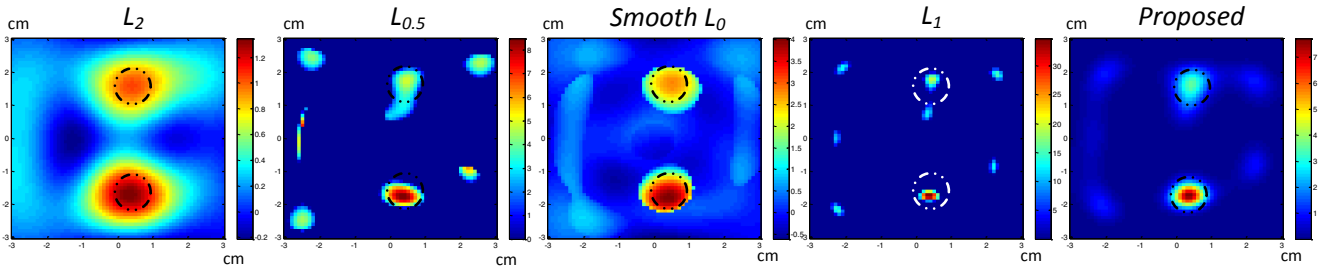

Fig. 4. Reconstructed images of two separated absorbers. Dashed circles indicate the actual size of the objects.

6. REFERENCES

[1] N. Cao, A. Nehorai, and M. Jacobs, "Image reconstruction for diffuse optical tomography using sparsity regularization and expectation-maximization algorithm," *Opt. Express*, vol. 15, pp. 13695–13708, 2007.

[2] J.C. Ye, S.Y. Lee, and Y. Bresler, "Exact reconstruction formula for diffuse optical tomography using simultaneous sparse representation," in *Proc. ISBI*, 2008.

[3] M. Süzen, A. Giannoula, and T. Durduran, "Compressed sensing in diffuse optical tomography," *Opt. Express*, vol. 18, no. 23, pp. 23676–23690, 2010.

[4] J. Prakash, C. Shaw, R. Manjappa, R. Kanhirodan, and P. K. Yalavarthy, "Sparse recovery methods hold promise for diffuse optical tomographic image reconstruction," *IEEE J. Sel. Topics Quantum Electron., to appear*, 2013.

[5] D. Donoho, "Compressed sensing," *IEEE Trans. Inf. Theory*, vol. 52, no. 4, pp. 1289–1306, 2006.

[6] B. K. Hölzel, U. Ott, H. Hempel, A. Hackl, K. Wolf, R. Stark, and D. Vaitl, "Differential engagement of anterior cingulate and adjacent medial frontal cortex in adept meditators and non-meditators," *Neurosci. Lett.*, vol. 421, no. 1, pp. 16–21, 2007.

[7] J. Huang, T. Zhang, and D. Metaxas, "Learning with structured sparsity," in *Proc. ICML*, 2009.

[8] V. Cevher, P. Indyk, C. Hegde, and R.G. Baraniuk, "Recovery of clustered sparse signals from compressive measurements," in *Proc. SAMPTA*, 2009.

[9] A. Beck and M. Teboulle, "A fast iterative shrinkage-thresholding algorithm for linear inverse problems," *SIAM J. Imag. Sci.*, vol. 2, no. 1, pp. 183–202, 2009.

[10] F. Tian, G. Alexandrakis, and H. Liu, "Optimization of probe geometry for diffuse optical brain imaging based on measurement density and distribution," *Appl. Opt.*, vol. 48, no. 13, pp. 2496–2504, 2009.

[11] P. C. Hansen and D. P. O'Leary, "The use of the L-curve in the regularization of discrete ill-posed problems," *SIAM J. Sci. Comput.*, vol. 14, no. 6, pp. 1487–1503, 1993.

[12] L. Jacob, G. Obozinski, and J. Vert, "Group lasso with overlap and graph lasso," in *Proc. ICML*, 2009.

[13] J Huang, S. Zhang, H. Li, and D. Metaxas, "Composite splitting algorithms for convex optimization," *Comput. Vis. Image Und.*, vol. 115, no. 12, pp. 1610–1622, 2011.

[14] P.Y. Chen and I.W. Selesnick, "Translation-invariant shrinkage/thresholding of group sparse signals," *Signal Process.*, vol. 94, pp. 476–489, 2014.

[15] D. Boas, D. Brooks, R. Gaudette, T. Gaudette, E. Miller, and Q. Zhang, "Photon migration imaging (PMI) toolbox," *http://www.nmr.mgh.harvard.edu/PMI/toolbox/*.

[16] H. Niu, F. Tian, Z. Lin, and H. Liu, "Development of a compensation algorithm for accurate depth localization in diffuse optical tomography," *Opt. Lett.*, vol. 35, no. 3, pp. 429–431, 2010.

[17] J. Huang, X. Huang, and D. Metaxas, "Learning with dynamic group sparsity," in *Proc. ICCV*, 2009.

[18] C. Chen and J. Huang, "Compressive Sensing MRI with Wavelet Tree Sparsity," in *Proc. of NIPS*, 2012.

[19] C. Chen and J. Huang, "The benefit of tree sparsity in accelerated MRI," *Med. Image Anal.*, 2014.

[20] J. Huang, C. Chen, and L. Axel, "Fast Multi-contrast MRI Reconstruction," in *Proc. of MICCAI*, 2012.